Determination of molecular vibrational state energies using the *ab initio* semiclassical initial value representation: Application to formaldehyde

Stephanie Y. Y. Wong,[1] David M. Benoit,[2] Marius Lewerenz,[3] Alex Brown,[1,a)] and Pierre-Nicholas Roy[4,b)]

[1]*Department of Chemistry, University of Alberta, Edmonton, Alberta T6G 2G2, Canada*
[2]*Nachwuchsgruppe Theorie, SFB 569, Albert-Einstein-Allee 11, University of Ulm, D-89081 Ulm, Germany*
[3]*Laboratoire Modelisation et Simulation, Multi Echelle (MSME FRE3160 CNRS), Université Paris Est (Marne-la-Vallée), Bâtiment Lavoisier, Cite Descartes, Champs sur Marne, 77454 Marne la Vallée Cedex 2, France*
[4]*Department of Chemistry, University of Waterloo, Waterloo, Ontario N2L 3G1, Canada*

(Received 13 December 2010; accepted 18 January 2011; published online 3 March 2011)

We have demonstrated the use of *ab initio* molecular dynamics (AIMD) trajectories to compute the vibrational energy levels of molecular systems in the context of the semiclassical initial value representation (SC-IVR). A relatively low level of electronic structure theory (HF/3-21G) was used in this proof-of-principle study. Formaldehyde was used as a test case for the determination of accurate excited vibrational states. The AIMD-SC-IVR vibrational energies have been compared to those from curvilinear and rectilinear vibrational self-consistent field/vibrational configuration interaction with perturbation selected interactions-second-order perturbation theory (VSCF/VCIPSI-PT2) and correlation-corrected vibrational self-consistent field (cc-VSCF) methods. The survival amplitudes were obtained from selecting different reference wavefunctions using only a single set of molecular dynamics trajectories. We conclude that our approach is a further step in making the SC-IVR method a practical tool for first-principles quantum dynamics simulations. © *2011 American Institute of Physics*. [doi:10.1063/1.3553179]

I. INTRODUCTION

Molecular dynamics (MD) simulations are classical investigations of the nuclear degrees of freedom where the electronic part of a molecular system is treated simply as an effective "force" term which is an integral component in the nuclear equations of motion. Traditionally, the force is obtained from an empirically derived potential energy surface (PES) or from a PES fit to single-point quantum mechanical calculations. *Ab initio* molecular dynamics (AIMD), or so-called "direct dynamics," simulations[1] are those where the forces are calculated "on the fly" without the need for a PES, making them amenable to a broad range of problems. The AIMD approach is powerful due to the unnecessary need to produce a predetermined PES, of which it is impractical to obtain for problems involving more than a small number of vibrational degrees of freedom. In cases where there are nonadiabatic effects or bond breaking/formation, the *ab initio* approach is particularly useful. AIMD can represent classical phenomena correctly, within the accuracy of the integrator and the chosen *ab initio* electronic structure method.

Classical MD simulations are successful in many situations where quantum effects are negligible or not of interest. However, when quantum effects are important, standard MD fails. Properties such as molecular energy states, interference, and coherence are nonclassical phenomena and are computed from quantum mechanical equations or their isomorphic equivalent, the path integral. The difficulty with solving quantum mechanical equations directly is that of exponential scaling. Therefore, a variety of different approaches have been suggested to circumvent this scaling problem. Depending on the method, certain properties are more easily attainable (or accurate) than others. For example, one may use the multiconfiguration time-dependent Hartree (MCTDH) (Refs. 2, 3, and 4) approach to approximate the full quantum mechanical solution. While a very powerful approach, the MCTDH method in general necessitates a full-dimensional PES fit to product form and, hence, has only been used for modest-sized systems of three to seven atoms. MULTIMODE (Refs. 3 and 5) is another software code that can calculate rovibrational energies of polyatomic molecules by using vibrational self-consistent field (VSCF) and vibrational configuration interaction (VCI). From the path integral formulation, the diffusion Monte Carlo (DMC) (Ref. 6) method can obtain ground state properties to very good accuracy. Its basis is the expression of the solution to the Schrödinger equation as a sum of exponentials in imaginary time. Unfortunately, DMC works only when the wavefunction is positive, meaning any wavefunction which has nodes (i.e., excited states) will not work. To deal with node-crossing in DMC, one has to apply a fixed-node approach where each region of the wavefunction is treated separately[7] [node-release DMC (Ref. 8) is a variant]. Ring polymer molecular dynamics (RPMD) is another method which can compute dynamical properties. One can then obtain real-time Kubo-transformed time-correlation functions.[9] In practice, however, as system size increases, these methods may become intractable, as

a)Electronic mail: alex.brown@ualberta.ca.
b)Electronic mail: pnroy@uwaterloo.ca.

either basis set, dimensionality or convergence issues multiply. For example, we are often limited to use pair potentials for DMC and RPMD or require a full-dimensional PES.

Semiclassical dynamics is another method for obtaining quantum-mechanical properties by representing the system in terms of definite positions and momenta.[10] The framework of computation is then classical. The semiclassical propagator developed by van Vleck[11] has been the basis of many practical advancements in semiclassical theory[12–14] and has been recently reviewed by Thoss and Wang[15] and by Kay.[16] In particular, a semiclassical initial value representation (SC-IVR) propagator was developed in 1984 by Herman and Kluk,[17] see also (Refs. 18, 19), which expresses the quantum time-propagation correlation function as a semiclassical expression in terms of coherent states. Unlike its predecessors,[11,12] an initial value representation eliminates root search and singularity problems. Instead of finding all possible *paths* between two coordinate-space points, one only needs initial-value information. This means the use of classical molecular dynamics *trajectories* is possible. The only other information required in addition to the classical trajectory itself is Hessian information from the dynamics.

In the last decade many developments in the SC-IVR method have been undertaken.[20–35] Among them have been prescriptions for the calculation of vibrational states,[24,29,32–36] vibronic absorption spectra,[26] reactive processes,[21] and quantum coherence.[27] Recently, two research groups have been involved in investigating *ab initio* SC-IVR, where the trajectories are calculated on the fly. Tatchen and Pollak[26] computed the absorption spectrum of the $S_0 \rightarrow S_1$ transition of formaldehyde using the time-dependent density functional theory (TD-DFT) (Ref. 37) method with the Perdew–Burke–Ernzerhof (PBE) (Ref. 38) functional. They used a unity-valued Herman–Kluk (HK) prefactor (see Sec. II for definition) to calculate the Herzberg–Teller correlation function. Most recently, Aspuru-Guzik and co-workers[28,29] employed AIMD in the study of the vibrational states of CO_2, which can be computed from the quantum time autocorrelation function. Here, they used a variant of SC-IVR called *time-averaged* SC-IVR, which utilizes a significantly reduced number of trajectories. Comparisons were made to states determined from fitted potential surfaces and the accuracy of state energies was examined. There have also been a number of other studies based on fitted PESs using SC-IVR to examine molecular vibrational states. Kaledin and Miller[24,36] have obtained the vibrational states of H_2, H_2O, NH_3, CH_4, CH_2D_2 and H_2CO with SC-IVR as well as time-averaged SC-IVR.[24] Roy and coworkers[23,32–35] developed a reduced-dimensionality approach through Cartesian geometric constraints [applying it to Ar_3 and $(H_2O)_2$], which is amenable for the computation of larger systems.

The focus of this paper is to determine accurate molecular vibrational states through a semiclassical approach. Determination of vibrational state energies within the harmonic approximation is trivial for even very large systems. However, when anharmonic corrections are introduced, the computational effort is much more considerable. What is possible to do—through the use of classical-based dynamics—is to use spectral densities from *ab initio* SC-IVR to compute vibrational state energies. By incorporating terms accounting for probability amplitudes, SC-IVR reintroduces the quantum contribution into the classical simulation. In this paper, we provide further insight into *ab initio*-based SC-IVR using H_2CO as a model system and address several points that have not been considered in previous studies.[24,28,29,32–34,36] As opposed to time-averaged SC-IVR,[24] we use standard SC-IVR (i.e., full phase space averaging) and an approximation of the Herman–Kluk prefactor (see Sec. II for discussion). Previous work[36] has utilized reference wavefunctions chosen on the basis of symmetry, but here we separate them on a normal-mode basis. Careful analysis of the results as a function of the chosen reference wavefunction is done. We also demonstrate a practical tool for performing *ab initio* SC-IVR within the MOLECULAR MODELLING TOOLKIT (MMTK),[39] a molecular dynamics software package. The low-lying vibrational states of H_2CO are determined and compared to harmonic, quartic force field correlation-corrected vibrational self-consistent field (cc-VSCF),[40] direct cc-VSCF,[41–43] direct rectilinear-vibrational self-consistent field/vibrational configuration interaction with perturbation selected interactions-second-order perturbation theory (VSCF/VCIPSI-PT2) as well as reference direct *curvilinear*-VSCF/VCIPSI-PT2 method results.[44,45]

Section II presents a brief review of the mathematical formulation of SC-IVR. Section III covers the details regarding the computation of the spectral density of H_2CO. In Sec. III A, we introduce the electronic structure methods used to produce the *ab initio* energies and frequencies. The most important component of the method is the phase space integral, which is obtained from the classical dynamics trajectories, as detailed in Sec. III B. The final spectral density depends largely on the reference wavefunction and so the prescription for determining the reference wavefunction and its overlaps are discussed in Sec. III C. Results and discussion of the obtained vibrational states follow in Sec. IV. Section V presents our final conclusions.

II. THEORY

The quantum mechanical survival amplitude is defined as

$$C(t) = \langle \Psi | e^{-i\hat{H}t/\hbar} | \Psi \rangle \tag{1}$$

and represents the correlation between a wavefunction at initial time $t = 0$ with itself at time t. Ψ is an arbitrary reference wavefunction and will from now on be denoted as Ψ_{ref}. The quantum propagator $e^{-i\hat{H}t/\hbar}$ determines the time-evolution of a molecular system. Within the SC-IVR approach, the quantum propagator can be replaced with the semiclassical Herman–Kluk propagator:[17–19,46]

$$e^{-i\hat{H}t/\hbar} = (2\pi\hbar)^{-3N} \int\int d\mathbf{p}_0 d\mathbf{q}_0 R_{\mathbf{p}_0,\mathbf{q}_0,t} e^{iS_{\mathbf{p}_0,\mathbf{q}_0,t}/\hbar} \times |g_{\mathbf{p}_t,\mathbf{q}_t}\rangle\langle g_{\mathbf{p}_0,\mathbf{q}_0}|. \tag{2}$$

The integrals are over the mass-weighted phase space variables, $\mathbf{p}_0$ and $\mathbf{q}_0$, and are determined through Monte

Carlo sampling. $|g_{\mathbf{p}_t,\mathbf{q}_t}\rangle$ and $\langle g_{\mathbf{p}_0,\mathbf{q}_0}|$ are coherent state representations of the minimum-uncertainty wavepacket, which is a multivariate Gaussian function of coherent-state width[13,17,47]

$$\gamma = 2L\alpha L^T, \tag{3}$$

where L is the eigenvector matrix and α is the eigenvalue matrix from the Hessian evaluated at the potential minimum. Coherent states have the property that the center of the Gaussian evolves according to the classical equations of motion. Both the coherent states at the initial (0) and current (t) times are required. $R_{\mathbf{p}_0,\mathbf{q}_0,t}$ represents the Herman–Kluk prefactor, a stability matrix. $S_{\mathbf{p}_0,\mathbf{q}_0,t}$ is the classical action, specifying the phase of the Gaussian wavepacket.

In this paper, we do not use the exact form[17] of the Herman–Kluk prefactor:

$$R_{\mathbf{p}_0,\mathbf{q}_0,t} = \sqrt{\det\left[\frac{1}{2}\left(\frac{\partial \mathbf{q}_t}{\partial \mathbf{q}_0} + \frac{\partial \mathbf{p}_t}{\partial \mathbf{p}_0} - i\hbar\gamma\frac{\partial \mathbf{q}_t}{\partial \mathbf{p}_0} + \frac{i}{\gamma\hbar}\frac{\partial \mathbf{p}_t}{\partial \mathbf{q}_0}\right)\right]}, \tag{4}$$

which is a determinant of monodromy stability matrices, requiring the derivatives of the time-evolved $(\mathbf{p}_t, \mathbf{q}_t)$ variables with respect to the initial variables $(\mathbf{p}_0, \mathbf{q}_0)$. In the present work, we use a locally quadratic approximation for the HK prefactor, i.e.,

$$R_{\mathbf{p}_0,\mathbf{q}_0,t} = \exp\left[-\frac{i}{\hbar}\int_0^t dt' \sum_{j=1}^{3N-6}\frac{\hbar\omega_j(t')}{2}\right]. \tag{5}$$

Note that Miller and co-workers refer to this expression as the "Johnson multichannel WKB approximation."[48,49] We adopt the same terminology as Miller for the remainder of this paper. In Eq. (5), ω_j corresponds to the angular frequency of each vibrational mode j at time t'. This is the *local* harmonic frequency (a frequency calculation not necessarily at a stationary point) of each timestep of the trajectory. It may be calculated at the same time as the dynamics step, reducing the electronic structure calculation overhead. This prefactor has been successfully used in studies of the vibrational states of weakly bound trimers and the water dimer.[32–35]

The phase term, $e^{iS_{\mathbf{p}_0,\mathbf{q}_0,t}/\hbar}$, comes from the Lagrangian equations of motion. The classical action S is the time-integral of the Lagrangian along the trajectory:

$$S_{\mathbf{p}_0,\mathbf{q}_0,t} = \int_0^t dt'\left(\frac{\mathbf{p}_{t'}^2}{2\mathbf{m}} - V(\mathbf{q}_{t'})\right). \tag{6}$$

The use of classical trajectories implies a Stationary Phase Approximation.

Combining Eqs. (1) and (2), we obtain a semiclassical expression for the survival amplitude, i.e.,

$$C(t) = (2\pi\hbar)^{-3N}\int\int d\mathbf{p}_0 d\mathbf{q}_0 R_{\mathbf{p}_0,\mathbf{q}_0,t} e^{iS_{\mathbf{p}_0,\mathbf{q}_0,t}/\hbar} \times\langle\Psi_{\text{ref}}|g_{\mathbf{p}_t,\mathbf{q}_t}\rangle\langle g_{\mathbf{p}_0,\mathbf{q}_0}|\Psi_{\text{ref}}\rangle, \tag{7}$$

where the overlap of Ψ_{ref} with the coherent state produces

$$\langle g_{\mathbf{p},\mathbf{q}}|\Psi_{\text{ref}}\rangle = \exp\left[-\frac{1}{4}(\mathbf{q}-\mathbf{q}_{\text{ref}})^T\gamma(\mathbf{q}-\mathbf{q}_{\text{ref}}) - \frac{1}{4\hbar^2} \times(\mathbf{p}-\mathbf{p}_{\text{ref}})^T\gamma^{-1}(\mathbf{p}-\mathbf{p}_{\text{ref}}) + \frac{i}{2\hbar}(\mathbf{p}+\mathbf{p}_{\text{ref}})^T(\mathbf{q}-\mathbf{q}_{\text{ref}})\right]. \tag{8}$$

$\mathbf{p}_{\text{ref}}$ and $\mathbf{q}_{\text{ref}}$ are the reference state mass-weighted momenta and positions, respectively. γ in this equation takes on the same values as in Eq. (3). The overlaps have a general Gaussian form. The reference state constitutes a chosen "trial" wavefunction, which is the desired state of interest. $C(t)$ is the correlation of the state of the system with this reference function, meaning the chosen reference function serves as an "extractor" for eigenstates near it. Note that in practice, the above overlap is also symmetry-adapted, which will be explained in Sec. III C.

When Eq. (7) is Fourier-transformed, the resultant power spectrum produces the energy eigenvalues of the Hamiltonian $\hat{H}$:

$$I(\omega) = \frac{1}{2\pi}\int_{-\infty}^{\infty} dt\, e^{i\omega t}C(t), \tag{9}$$

with the intensities of the peaks directly related to the choice of reference wavefunction.

III. COMPUTATIONAL METHODS

A. Electronic structure and harmonic frequencies

In order to benchmark our SC-IVR approach, the *ab initio* electronic structure calculations were carried out at the HF/3-21G level of theory.[50,51] The equilibrium geometry is given in Table I. Energies at which the simulation is run are far below than that of the HF transition state (37 700 cm^{-1}).[52] The availability of analytic gradients and Hessians, required for the classical dynamics and HK prefactor evaluation, respectively, is a major asset and guided, along with its computational efficiency, the choice of the Hartree–Fock level of theory. In principle, any electronic structure theory methodology, for which analytic gradients and Hessians are available, could be utilized. Our calculations made use of the GAMESS-US 2007 and 2009 quantum chemistry packages.[53]

TABLE I. Equilibrium geometry of H_2CO at the HF/3-21G level of theory. Bond lengths are given in Angstrom (Å) and the bond angle in degrees (°).

Parameter	Value
r_{CO}	1.207
r_{CH}	1.083
θ_{HCO}	122.5

B. Trajectories for phase space average

To determine the initial conditions for the ensemble of trajectories, a Monte Carlo sampling of $M = 20\,000$ sets of initial geometric configurations and momenta was produced, corresponding to a coherent state Gaussian wavepacket centered at the HF/3-21G equilibrium geometry and with zero momentum. This phase space sampled represents $|\langle g_{\mathbf{p}_0,\mathbf{q}_0}|\Psi_{\rm eq}\rangle|^2$, whose form is identical to that of Eq. (8). The coordinate and momentum widths of Eq. (8) are $\sqrt{2/\gamma}$ and $\hbar\sqrt{2\gamma}$, respectively. Of these initial conditions, only motion in the $3N-6$ internal degrees of freedom is allowed, and so the original values are adjusted, fixing the molecule's center of mass and spatial orientation. Note that only one set of initial conditions is used for the various reference wavefunctions and therefore, a reweighting procedure is required. Equation (7) can be rewritten with the insertion of unity $\mathbb{1} = |\langle g_{\mathbf{p}_0,\mathbf{q}_0}|\Psi_{\rm eq}\rangle|^2/|\langle g_{\mathbf{p}_0,\mathbf{q}_0}|\Psi_{\rm eq}\rangle|^2$ as

$$C(t) = (2\pi\hbar)^{-3N}\iint d\mathbf{p}_0 d\mathbf{q}_0 R_{\mathbf{p}_0,\mathbf{q}_0,t} e^{iS_{\mathbf{p}_0,\mathbf{q}_0,t}/\hbar} \times \langle\Psi_{\rm ref}|g_{\mathbf{p}_t,\mathbf{q}_t}\rangle\langle g_{\mathbf{p}_0,\mathbf{q}_0}|\Psi_{\rm ref}\rangle \frac{|\langle g_{\mathbf{p}_0,\mathbf{q}_0}|\Psi_{\rm eq}\rangle|^2}{|\langle g_{\mathbf{p}_0,\mathbf{q}_0}|\Psi_{\rm eq}\rangle|^2}. \quad (10)$$

The initial conditions essentially impose a bias of $|\langle g_{\mathbf{p}_0,\mathbf{q}_0}|\Psi_{\rm eq}\rangle|^2$ (the numerator in $\mathbb{1}$) in the phase space distribution which must be accounted for by division of the bias. The Monte Carlo estimate is therefore

$$C(t) = \frac{1}{M}\sum_{m=1}^{M}\left[R_{\mathbf{p}_0,\mathbf{q}_0,t} e^{iS_{\mathbf{p}_0,\mathbf{q}_0,t}/\hbar}\frac{\langle\Psi_{\rm ref}|g_{\mathbf{p}_t,\mathbf{q}_t}\rangle\langle g_{\mathbf{p}_0,\mathbf{q}_0}|\Psi_{\rm ref}\rangle}{\langle\Psi_{\rm eq}|g_{\mathbf{p}_0,\mathbf{q}_0}\rangle\langle g_{\mathbf{p}_0,\mathbf{q}_0}|\Psi_{\rm eq}\rangle}\right]_m. \quad (11)$$

This choice of sampling greatly reduces the computational cost as only one set of *ab initio* trajectories is required instead of a full phase space distribution.

Approximately 38% of the 20 000 generated initial geometries and momenta had a total energy less than 300 kJ/mol (~25 000 cm^{-1}). Initial conditions with energies above 300 kJ/mol were discarded. Energies below 300 kJ/mol place the molecule well below the transition state, which is important in the numerical stability of the Herman–Kluk prefactor. Additionally, the semiclassical survival amplitude, $C(t)$, was computed only when $|\langle g_{\mathbf{p}_0,\mathbf{q}_0}|\Psi_{\rm eq}\rangle|^2 > 10^{-10}$. Low overlap leads to negligible contribution to the average of the survival amplitude. From each of these initial conditions, a 244 fs constant energy molecular dynamics trajectory was determined using MMTK.[39] These trajectories constitute the phase space average, which is the multidimensional integral in $C(t)$. The equations of motion were computed with Velocity-Verlet[54] integration. During the dynamics, the Hessian at each timestep (0.5 fs) is saved and diagonalized. The resultant eigenvalues are necessary for the calculation of the HK prefactor which requires the local harmonic zero point energy [see Eq. (5)].

C. Reference wavefunctions and overlaps

The coherent state overlaps are functions of mass-weighted geometry and momentum. A choice of reference wavefunction where $\mathbf{q}_{\rm ref}$ is located at the equilibrium geometry and $\mathbf{p}_{\rm ref} = 0$, will produce the highest overlap with the lowest vibrational state (zero point energy). In all cases we choose $\mathbf{p}_{\rm ref}$ to be zero, for simplicity, and we vary only $\mathbf{q}_{\rm ref}$. The width is chosen to be γ as previously defined, meaning that $\Psi_{\rm ref}$ is the exact harmonic ground state wavefunction, and there is no appreciable overlap with any state other than the ground state. When another reference wavefunction is chosen, it will be those coherent states (i.e., phase space points along the trajectory) which have highest overlap with this wavefunction that will contribute the most to the survival amplitude. One way to vary the wavefunction in order to obtain additional states is to apply a technique where the atoms are spatially displaced along a normal mode coordinate. As a result, it is easy to interpret the magnitude of displacement (c) with the energy put "into" a mode ν_j (in this work, we use ν to denote the mode itself). For instance, by letting $c = \sqrt{\hbar/\omega_j}$ displacement of mode ν_j, this means that the molecule has been displaced from equilibrium along ν_j and thus has $1/2(\hbar\omega_j)$ of potential energy (assuming the motion is perfectly harmonic). Essentially, this provides an excited state reference wavefunction. The normal modes are as assigned in Table II. By allowing just single normal mode displacements, this should effectively produce a spectrum with peaks only at the fundamental frequencies and overtones, i.e., $(n_1 \cdots n_j \cdots n_N) : n_{j\neq k} = 0, n_k \in \mathbb{Z}_{>0}$.

TABLE II. Harmonic normal mode labeling and frequencies (cm^{-1}). Frequencies are determined at the HF/3-21G level of theory.

Mode	Assignment	Frequency
ν_1(A1)	CH_2 symmetric stretch	3162
ν_2(A1)	CO stretch	1916
ν_3(A1)	CH_2 scissor	1693
ν_4(B1)	CH_2 wag	1337
ν_5(B2)	CH_2 asymmetric stretch	3233
ν_6(B2)	CH_2 rock	1378

A Monte Carlo procedure is used to estimate the phase space integrals and therefore, all eigenstates could contribute to the survival amplitudes. The normal mode displacements in the reference wavefunction are also not pure symmetry states. To remedy this problem, we explicitly symmetrize the reference wavefunction. To do so, we project out specific symmetries by constructing a projection operator corresponding to a specific irreducible representation of the C_{2v} group. For the case of symmetric A_1 states, an unsymmetrized reference wavefunction, $|\Psi_{\rm ref}\rangle$, becomes,

$$|\Psi_{\rm ref}^{A_1}\rangle = \frac{1}{4}\left[\hat{E}|\Psi_{\rm ref}\rangle + \hat{C}_2|\Psi_{\rm ref}\rangle + \hat{\sigma}_v|\Psi_{\rm ref}\rangle + \hat{\sigma}_v'|\Psi_{\rm ref}\rangle\right]. \quad (12)$$

The use of the above wavefunction will ensure that energy levels of a specific symmetry are extracted (cf. Ref. 36, where a product of coherent states is used instead, with a symmetrizer to extract states of particular molecular symmetry).

Because the width γ [see Eq. (3)] is identical to that of the ground state wavefunction, one may visualize the displaced reference wavefunction (prior to symmetrization) as simply a

shift of the ground state wavefunction along a single normal mode coordinate. For a given mode j, the new atom positions in Cartesian coordinates is represented as the vector x^j (we call this x to differentiate this from the mass-weighted coordinate q). For each individual coordinate α, the elements of the vector x^j are:

$$x_\alpha^j = X_\alpha - c_j \frac{L_{\alpha j}}{\mu_\alpha}, \tag{13}$$

where X_α is an element of the Cartesian equilibrium geometry vector, μ_α is the square root of the mass of the atom associated with Cartesian component α, and $L_{\alpha j}$ is the eigenvector element associated with displaced mode ν_j. In this work, c_j is varied by factor d to adjust the magnitude of the normal mode displacement ($c_j = d \cdot \sqrt{\hbar/\omega_j}$).

D. Reference bound state calculations

To determine the accuracy of the semiclassical results, we used a number of computational methods for comparison: correlation-corrected vibrational self-consistent field/two-mode coupling representation of a quartic force field (cc-VSCF/2MR-QFF), direct cc-VSCF, VSCF/VCIPSI-PT2, and curvilinear-VSCF/VCIPSI-PT2.

The VSCF procedure provides a variational solution to the vibrational Schrödinger equation.[55,56] It uses a separable product of one-coordinate functions to represent the total vibrational wavefunction, such that

$$\Phi_{\mathbf{n}}(\mathbf{Q}) = \prod_{j=1}^{N} \varphi_{n_j}^{(\mathbf{n})}(Q_j), \tag{14}$$

where ($\mathbf{n}$) is a collective index representing the vibrational state of interest, be it the ground state or any singly excited state, overtone, or combination band. GAMESS-US (Ref. 53) implements a correlation-corrected VSCF where the potential energy surface including up to two-mode couplings can either be computed using a quartic force field (cc-VSCF/2MR-QFF) (Ref. 40) or by computing the PES on a grid using single-point calculations (direct cc-VSCF).[42]

In the methodology developed by Benoit and coworkers,[44,45] a variation-perturbative approach, perturbative screening is used to iteratively update the initial vibrational configuration interaction active space (VSCF/VCIPSI-PT2). This calculation can be performed for a PES expressed either in rectilinear or curvilinear coordinates (curvilinear-VSCF/VCIPSI-PT2), which lends to more efficient computation. The advantage of using curvilinear coordinates is that it is amenable to systems of multiple local minima and that it reduces mode–mode coupling, leading to a more accurate representation of the vibrational states. Rectilinear coordinates, on the contrary, often expand the wavefunction over a single minimum and can introduce artificially large mode–mode couplings. The curvilinear-VSCF/VCIPSI-PT2 vibrational states are used as our reference values.

In the current implementation (see Ref. 45 for details), the set of curvilinear coordinates $\mathbf{q}$ is transformed into curvilinear normal mode coordinates, $\mathbf{Q}$. The corresponding metric tensor is constant and reduced to an identity operator δ_{ij}. The application of the variational principle to the resulting Hamiltonian:

$$\hat{\mathbf{H}} = -\frac{1}{2}\sum_{j=1}^{N}\frac{\partial^2}{\partial Q_j^2} + \underbrace{\sum_{j=1}^{N} V_j^{(1)}(Q_j) + \sum_{i=1}^{N}\sum_{j>i}^{N} V_{ij}^{(2)}(Q_i, Q_j)}_{V(\mathbf{Q})} \tag{15}$$

leads naturally to N one-dimensional equations

$$\left\{ -\frac{1}{2}\frac{\partial^2}{\partial Q_j^2} + V_j^{(1)}(Q_j) + \vartheta_j^{(\mathbf{n})}(Q_j) \right\} \varphi_{n_j}^{(\mathbf{n})}(Q_j) = \epsilon_{n_j}^{(\mathbf{n})} \varphi_{n_j}^{(\mathbf{n})}(Q_j) \tag{16}$$

that are coupled through a mean-field potential

$$\vartheta_j^{(\mathbf{n})}(Q_j) = \left\langle \prod_{i\neq j} \varphi_{n_i}^{(\mathbf{n})} \middle| \sum_{i\neq j}^{N} V_{ij}^{(2)}(Q_i, Q_j) \middle| \prod_{i\neq j} \varphi_{n_i}^{(\mathbf{n})} \right\rangle. \tag{17}$$

The last two terms of the right-hand side of Eq. (15) are a representation of the potential energy surface as a hierarchical expansion to second-order in curvilinear normal modes. Each term of the potential expansion is computed on a grid of points (direct approach), providing a simple and automatic way of generating the PES directly from *ab initio* data without requiring an analytic expression for $V(\mathbf{Q})$. Note that, for a curvilinear coordinate system, an extra potential term may appear in the kinetic energy operator when a non-Euclidian normalization convention is used. In the present study, we neglect this contribution as it is typically very small compared to the potential energy term.

The set of Eq. (16) are solved self-consistently until convergence of the total VSCF energy. We then compute the correlated vibrational eigenstates by diagonalizing the full Hamiltonian of Eq. (15) in a virtual VSCF basis, as suggested originally by Bowman *et al.*[57–59] We perform this type of VCI calculation for each VSCF-optimized state and use virtual excitations to construct the VCI matrix in each case:

$$\langle \Phi_{\mathbf{r}} | \hat{\mathbf{H}} | \Phi_{\mathbf{s}} \rangle = \sum_{i=1}^{N} \epsilon_{r_i} \prod_{k\neq i} \delta_{r_k s_k} + \langle \Phi_{\mathbf{r}} | \Delta V^{(\mathbf{n})} | \Phi_{\mathbf{s}} \rangle, \tag{18}$$

where the state-specific vibrational correlation operator, $\Delta V^{(\mathbf{n})}$ is defined as

$$\Delta V^{(\mathbf{n})} = \sum_{i=1}^{N}\sum_{j>i}^{N} V_{ij}^{(2)}(Q_i, Q_j) - \sum_{j=1}^{N} \vartheta_j^{(\mathbf{n})}(Q_j). \tag{19}$$

Note that index ($\mathbf{n}$) indicates that the effective potential is computed for optimized VSCF state $|\Phi_{\mathbf{n}}\rangle$. The resulting VCI matrix is diagonalized using our iterative VCIPSI-PT2 procedure based on a Davidson algorithm[60–62] adapted for vibrational calculations by Carter *et al.*[59]

IV. RESULTS AND DISCUSSION

Here we present the results of the calculation of the spectral density of H_2CO as determined by SC-IVR. The peaks of

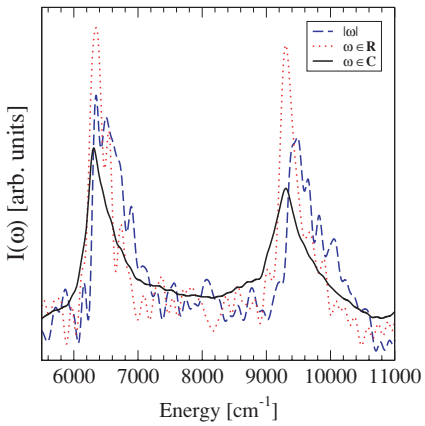

FIG. 1. Variation of the spectral density (displaced in ν_1) with respect to the type of HK prefactor used. The dashed (blue) line indicates use of the absolute value of ω, the dotted (red) line sums only the positive frequencies and the solid (black) line has a complex-valued ω (no further approximations).

the spectral density are the low-lying vibrational eigenvalues. It is possible for SC-IVR to determine more states, albeit at a substantial cost of longer (and possibly more) trajectories. In this particular case, however, the correlation function decays to a great extent within the timespan of the simulation and so provides minimal difference in the spectra. Our goal is a proof-of-principle of our implementation of the *ab initio* SC-IVR approach, rather than a thorough determination of the eigenvalues of formaldehyde at the HF/3-21G level of theory. The symmetry-adapted reference wavefunction of Eq. (12) is used for all the SC-IVR results. The SC-IVR values are compared to the harmonic approximation, cc-VSCF/2MR-QFF, direct cc-VSCF, (rectilinear) VSCF/VCIPSI-PT2, and curvilinear-VSCF/VCIPSI-PT2 methods described earlier. While vibrational states in the harmonic approximation are trivially obtained to the nth state, anharmonic terms are increasingly difficult to compute. As a result, in all four VSCF implementations, only two-mode couplings were utilized and three-mode (and higher) couplings were neglected. In order to make sure that the VSCF results used in the VSCF/VCIPSI-PT2 methods are fully converged, we include up to four-mode excitations in the VCI basis and allow up to eight excitation quanta per mode. This leads to a large vibrational basis (about 70 000 states) that is more appropriate for describing combination bands and overtones. Given the large size of the basis, we performed the calculations with a slightly different technique than VCI called vibrational configuration interaction with perturbation selected interactions-second-order perturbation (VCIPSI-PT2). It has been shown[45] that this method gives virtually the same results as a standard VCI/VSCF calculation. Of the four reference calculation types being considered, the curvilinear approach is the most accurate.

As detailed in Sec. II, we use an alternate form of the Herman–Kluk prefactor. Johnson's approximation[48] has been shown to be effective for weakly bound systems.[32–35] This approximation eliminates branch cut problems as well as the need to calculate phase space derivatives. Instead, one only needs to calculate the Hessian matrix at each geometry along the trajectories. Diagonalization of the Hessian matrix gives the eigenvalues, whose square roots are the *local* harmonic frequencies. These ω_js are similar to frequencies calculated at stationary points (i.e., at the equilibrium or transition state geometries). Since the frequencies are calculated at any point on the potential energy surface they are naturally complex-valued. The result is a highly oscillatory exponential term that increases noise in the survival amplitude function. In Fig. 1, we present results comparing spectra obtained with Johnson's WKB approach along with several further approximations. Issack and Roy[32–35] took the approach of taking the absolute value of all the frequencies ($|\omega|$) to eliminate the oscillating phase. This simplification results in a larger magnitude term in the exponential of Eq. (5) since it is taking a sum over additional positive real numbers. The HK prefactor, $R_{\mathbf{p}_0,\mathbf{q}_0,t}$, becomes a larger negative complex exponent. This appears to lead to overestimating the energy of the vibrational states (see Fig. 1). As well, the decay of the survival amplitude is much slower (not illustrated). Alternatively, if one encounters an imaginary frequency, one can simply neglect it, so that only the real frequencies are taken into account ($\omega \in \mathbb{R}$). The different summations do provide minor differences in the spectral density, with the peak positions between $\omega \in \mathbb{R}$ and a complex ω being negligible. In fact, $\omega \in \mathbb{C}$ appears to reduce signal noise. However, the signal intensity of the peaks is slightly diminished compared to $\omega \in \mathbb{R}$. The

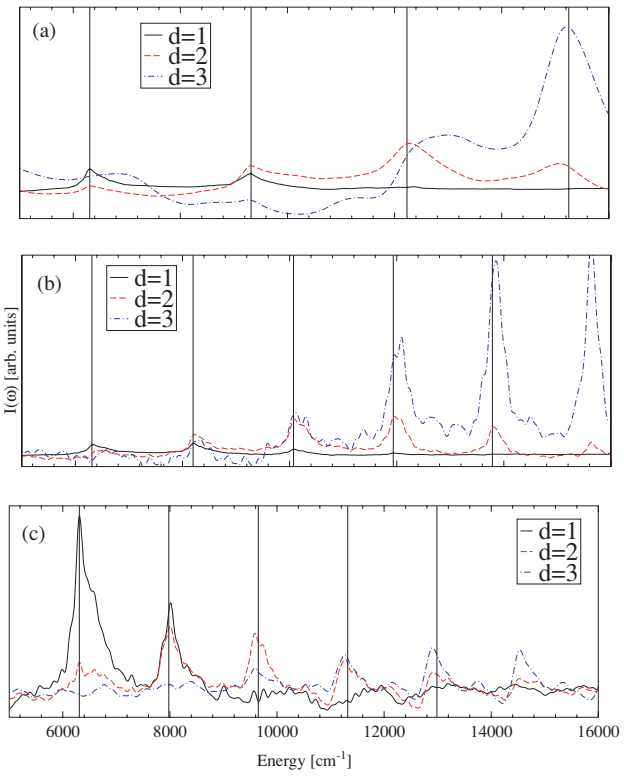

FIG. 2. Intensity (spectral density) plots from SC-IVR given symmetry-adapted reference state overlaps with displacements along the three A1 normal modes, (a) ν_1, (b) ν_2, and (c) ν_3, respectively. The curves are the SC-IVR results. d represents the magnitude of displacement (energy $\propto d^2$) of each mode (see text for details). The vertical lines represent the curvilinear-VSCF/VCIPSI-PT2 reference bound state calculation. In each panel, the left-most vertical line represents the ground vibrational state (000000), and in the case of the first panel, the subsequent lines are the (100000), (200000), (300000), and (400000) vibrational states. The other two panels are similarly labeled.

TABLE III. Fundamental vibrational states involving the A1 normal modes of H_2CO at the HF/3-21G level as determined using various computational methods. Units are in cm^{-1}. The SC-IVR values were determined by the location of the point of the highest intensity peak of one or more spectra (average), where each point was separated by < 0.5 cm^{-1}. The mean absolute error (MAE) and root mean square deviation (RMSD) with respect to the curvilinear-VSCF/VCIPSI-PT2 method are shown for the fundamental overtones.

State	Harmonic	cc-VSCF/2MR-QFF	Direct cc-VSCF	VSCF/VCIPSI-PT2	Curvilinear-VSCF/VCIPSI-PT2	SC-IVR
(000000)	6360	6271	6268	6268	6309	6311
(100000)	9522	9265	9254	9251	9320	9303
(010000)	8276	8155	8152	8152	8198	8208
(001000)	8053	7924	7922	7921	7980	8013
(200000)	12 685	12 183	12 136	12259	12232	12 297
(020000)	10 191	10 029	10 024	10023	10074	10 089
(002000)	9745	9574	9571	9571	9650	9587
(300000)	15 847	15 071	14 955	15103	15254	15 209
(030000)	12 107	11 893	11 885	11881	11936	11 961
(003000)	11 438	11 164	11 216	11216	11321	11 269
(400000)	19 010	—	17 721	17938	17996	17 848
(040000)	14 022	—	13 735	13727	13787	13 853
(004000)	13 131	—	12 851	12851	12986	12 904
MAE	257	74	104	72	—	48
RMSD	370	89	133	80	—	61

difference between the use of complex-, real-, or absolute-valued frequencies may be in the tens of wavenumbers, which may be significant for the accuracy of SC-IVR, although the width of the spectral peaks is comparable to the shift due to the type of prefactor. In the present work, we see no reason not to use the complex-valued frequencies, since there appears to be no benefit in simplifying the WKB approximation further (whether it is more difficult to converge the prefactor in other systems, such as weakly bound complexes, warrants further investigation). In all the following calculations we maintain the complex value of the frequencies ($\omega \in \mathbb{C}$). Note that all 12 eigenvalues of the Hessian are nonzero, including the rotational and translational modes. As seen in Eq. (5), the summation is only over $3N - 6$ modes (cf. previous literature), so the extraneous nonvibrational frequencies must be removed in the prefactor evaluation—we do so in the present work by neglecting the six lowest magnitude frequencies.

Following Sec. III C, we examine the spectral density as a function of the reference state chosen. We show the results of simulations with normal mode displacements along the A1

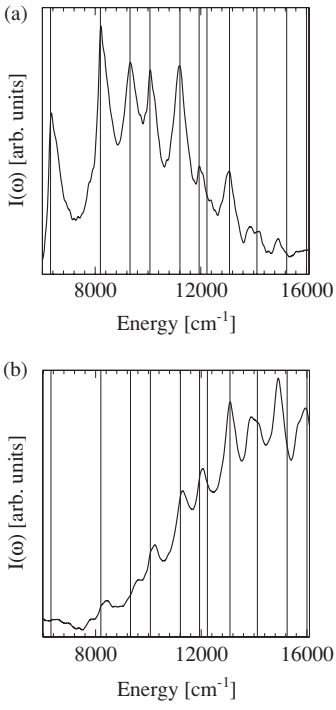

FIG. 3. Spectral density plots where the ν_1 and ν_2 A1 modes are displaced simultaneously when constructing the reference wavefunction. The vertical lines represent the reference curvilinear-VSCF/VCIPSI-PT2 values (see Table III for labeling) (a) $d = 1$ and (b) $d = 2$.

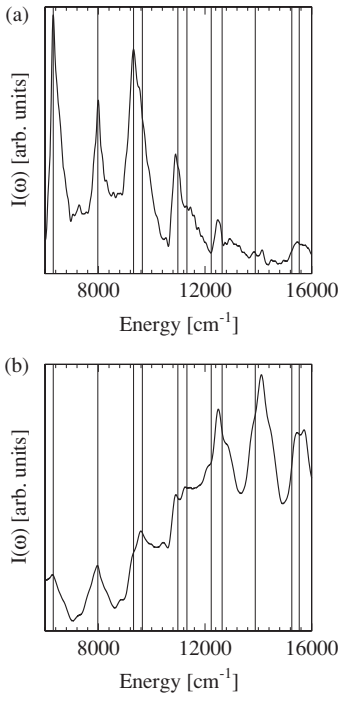

FIG. 4. Spectral density plots where the ν_1 and ν_3 A1 modes are displaced simultaneously when constructing the reference wavefunction. The vertical lines represent the reference curvilinear-VSCF/VCIPSI-PT2 values (see Table III for labeling) (a) $d = 1$ and (b) $d = 2$.

TABLE IV. Vibrational combination states involving the A1 normal modes of H_2CO at the HF/3-21G level as determined using various computational methods. Units are in cm^{-1}. The SC-IVR values were determined by the location of the point of the highest intensity peak of one or more spectra (average), where each point was separated by $< 0.5\ cm^{-1}$. Values with an asterisk (*) indicate that the assignment is uncertain.

State	Harmonic	cc-VSCF/2MR-QFF	Direct cc-VSCF	VSCF/VCIPSI-PT2	Curvilinear-VSCF/VCIPSI-PT2	SC-IVR
(110000)	11 438	11 164	11 133	11 126	11 211	11 191
(210000)	14 600	14 072	14 006	14 120	14 126	14 055*
(120000)	13 354	13 025	12 997	12 987	13 088	13 086
(220000)	16 516	—	15 860	15 967	16 004	15 952
(101000)	11 215	10 913	10 885	10 876	10 981	10 896
(201000)	14 377	13 795	13 735	13 844	13 884	14 115
(102000)	12 908	12 525	12 511	12 498	12 642	12 488*
(202000)	16 070	—	15 329	15 430	15 533	15 591*
(011000)	9968	9801	9805	9794	9858	9858
(021000)	11 884	11 665	11 672	11 653	11 722	11 690
(012000)	11 661	11 439	11 453	11 432	11 517	11 562
(022000)	13 576	—	13 316	13 279	13 370	13 544*

modes of vibration, ν_1, ν_2, and ν_3. Since the wavefunction is symmetry-adapted for A1, in theory, all A1 vibrational states should be obtained. Yet, as solely the A1 normal modes are excited, we only expect to obtain their fundamentals, overtones and, to a certain extent, their combination bands, the others being of negligible amplitude.

The spectral density as determined by SC-IVR is shown in Fig. 2. Three values of configurational displacement along the normal mode (magnitude specified by d), are shown. As can be seen, the further the reference wavefunction is displaced from the equilibrium geometry, the larger the overlap with higher energy states. Therefore, increasing the reference wavefunction displacement is a systematic way to determine vibrational states of increasing energy. The ground state (000000) is resolved in all figures. Each of the curves in Figs. 2(a), 2(b), and 2(c) resolves one set of vibrational states $(\cdots n \cdots)$ due the overlap with a single normal mode (in the harmonic limit). The benefit of such "filtering" is that a cleaner spectrum is obtained, so that close-lying eigenvalues are unequivocally differentiated. Spectral noise and uncertainty are major issues for many-dimensional systems and states of higher excitation. The intensities in Fig. 2(a) have the broadest peaks because the reference wavefunction energy (i.e., displacement) is largest (since it is proportional to ω_1). It is more difficult to extract states higher in energy (phase space coverage decreases, meaning the overlap term is often zero and therefore has no contribution to the overall survival amplitude integral). Table III lists the A1 fundamental and overtone vibrational state peak positions up to four-quanta excitation and also the mean absolute errors and root mean square deviations as compared to curvilinear-VSCF/VCIPSI-PT2. The assignments are quite close to the curvilinear bound state calculations (vertical lines) for low excitation, and, in general, are well within $100\ cm^{-1}$. As expected, errors and deviations become larger as one goes higher in energy. The results show that the SC-IVR results are systematically more accurate than that of the cc-VSCF/2MR-QFF (i.e., a VSCF-type method), direct cc-VSCF, and the rectilinear-VSCF/VCIPSI-PT2 (i.e., a VSCF/VCI method) results when compared to the more accurate curvilinear-VSCF/VCIPSI-PT2 reference calculations.

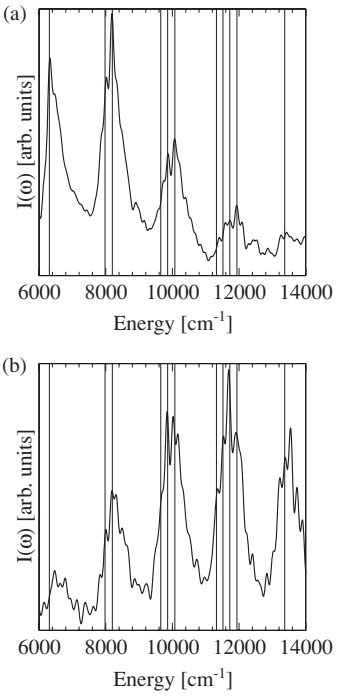

FIG. 5. Spectral density plots where the ν_2 and ν_3 A1 modes are displaced simultaneously when constructing the reference wavefunction. The vertical lines represent the reference curvilinear-VSCF/VCIPSI-PT2 values (see Table III for labeling) (a) $d = 1$ and (b) $d = 2$.

Figs. 3–5 show spectral densities consisting of reference state displacements of two modes simultaneously. That is, it is a linear combination of single mode displacements. Like those shown in Fig. 2, the fundamental bands are obtained, although with somewhat less accuracy. Many combination bands are also visible, although given the width of the peaks and that they are often near other states, assignments can be made with less certainty. In most cases, the location of the highest peak was the value tabulated in Table IV and if the peaks were clearly defined or equally ambiguous in more than one spectrum, the average of these locations were chosen. This uncertainty may be rectified with a more detailed procedure of displacing the reference wavefunction (here, we place

a single quanta of energy into each normal mode) and potentially increasing the number of trajectories involved in the calculation.

V. CONCLUDING REMARKS

We have shown, using *ab initio* trajectory data, that the vibrational eigenvalues of H_2CO can be determined with reasonable accuracy through the use of SC-IVR and that it is systematically more accurate than VSCF and VSCF/VCI methods. The curvilinear-VSCF/VCIPSI-PT2 bound state approach is used as our exact reference. Our semiclassical description comes at acceptable computational cost, but does have limitations. The vibrational states determined are highly sensitive to the reference wavefunction chosen. As such, for a complete description of a range of eigenvalues, multiple carefully constructed reference wavefunctions are required to extract them. In this work, we chose symmetry-adapted reference wavefunctions that had excitations along 1 or 2 normal modes only. This prescription allows us to independently and accurately determine fundamental states and some two-state combination bands of A1 symmetry. This symmetrizing enables easier assignment of states. The major bottleneck in these simulations is the trajectory and Hessian computation. However, once done, the phase space average for the survival amplitude is readily calculated. An important outcome of the present study is that in utilizing our newly proposed phase space reweighting procedure, only a *single* set of *ab initio* trajectories is required to obtain several power spectra.

In addition, we have examined the various implementations of Johnson's WKB approximation for the calculation of the HK prefactor. We have concluded that the local harmonic frequencies require no further simplification (i.e., can remain complex) since, at least in the case of H_2CO, it is not computationally advantageous. SC-IVR is an effective method for determining energy levels beyond the harmonic limit. However, it remains to be seen whether results would be as accurate for a more anharmonic system: at low energy, H_2CO is very harmonic. Therefore, the resolution of the data is a significant factor if the anharmonic correction for the eigenvalues lies within the width of the spectral peaks. As anharmonicity increases, it may also be more difficult to obtain accurate results due to the nature of the method (especially with the harmonic WKB approximation). However, previous results on the strongly anharmonic water dimer suggest that the approximation is reasonable.[34,35] The challenge in obtaining higher excitations is another limitation, yet the solution might be simply increasing the number of trajectories. How many more remains to be investigated. *Ab initio* SC-IVR appears promising for extracting some quantum effects in molecular systems and its practicality will be important for larger molecules where full quantum simulations are not currently possible.

ACKNOWLEDGMENTS

A.B., P.-N.R, and S.Y.Y.W. thank the Natural Sciences and Engineering Research Council of Canada (NSERC) for financial support and the Canadian Foundation for Innovation for funding for computational resources. This research has been (partially) enabled by the use of computing resources provided by WestGrid and Compute/Calcul Canada. S.Y.Y.W. thanks Dr. Bilkiss Issack for her input in the initial stages of the project as well as Dr. José-Luis Carreón-Macedo for development work and discussions in related efforts. S.Y.Y.W. acknowledges the support of NSERC through the award of an NSERC Canada Graduate Scholarship. This work was partly supported by a grant ("SFB-569/TP-N1") from the Deutsche Forschungsgemeinschaft (DFG) to D.M.B.

[1] R. Iftimie, P. Minary, and M. E. Tuckerman, Proc. Natl. Acad. Sci. U. S. A. **102**, 6654 (2005).
[2] H.-D. Meyer, U. Manthe, and L. S. Cederbaum, Chem. Phys. Lett. **165**, 73 (1990).
[3] J. M. Bowman, T. Carrington, and H.-D. Meyer, Mol. Phys. **106**, 2145 (2008).
[4] H.-D. Meyer, F. Gatti, and G. A. Worth, *Multidimensional Quantum Dynamics: MCTDH Theory and Applications* (Wiley-VCH, Weinheim, 2009).
[5] J. M. Bowman, S. Carter, and X. Huang, Int. Rev. Phys. Chem. **22**, 533 (2003).
[6] J. B. Anderson, J. Chem. Phys. **63**, 1499 (1975).
[7] P. J. Reynolds, D. M. Ceperley, B. J. Adler, and J. W.A. Lester, J. Chem. Phys. **77**, 5593 (1982).
[8] D. M. Ceperley and B. J. Adler, J. Chem. Phys. **81**, 5833 (1984).
[9] I. R. Craig and D. E. Manolopoulos, J. Chem. Phys. **121**, 3368 (2004).
[10] M. F. Herman, Annu. Rev. Phys. Chem. **45**, 83 (1994).
[11] J. H. van Vleck, Proc. Nat. Acad. Sci. U. S. A. **14**, 178 (1928).
[12] W. H. Miller, J. Chem. Phys. **53**, 3578 (1970)
[13] E. J. Heller, J. Chem. Phys. **75**, 2923 (1981).
[14] K. G. Kay, J. Chem. Phys. **100**, 4377 (1994).
[15] M. Thoss and H. Wang, Annu. Rev. Phys. Chem. **55**, 299 (2004).
[16] K. G. Kay, Annu. Rev. Phys. Chem. **56**, 255 (2005).
[17] M. F. Herman and E. Kluk, Chem. Phys. **91**, 27 (1984).
[18] W. H. Miller, Mol. Phys. **100**, 397 (2002).
[19] S. A. Deshpande and G. S. Ezra, J. Phys. A **39**, 5067 (2006).
[20] W. H. Miller, J. Phys. Chem. A **105**, 2942 (2001).
[21] X. Sun and W. H. Miller, J. Chem. Phys. **110**, 6635 (1999).
[22] W. H. Miller, J. Phys. Chem. A **113**, 1405 (2009).
[23] B. B. Harland and P.-N. Roy, J. Chem. Phys. **118**, 4791 (2003).
[24] A. L. Kaledin and W. H. Miller, J. Chem. Phys. **118**, 7174 (2003).
[25] J. M. Moix and E. Pollak, J. Chem. Phys. **129**, 64515 (2008).
[26] J. Tatchen and E. Pollak, J. Chem. Phys. **130**, 41103 (2009).
[27] G. Tao and W. H. Miller, J. Chem. Phys. **130**, 184108 (2009).
[28] M. Ceotto, S. Atahan, S. Shim, G. F. Tantardini, and A. Aspuru-Guzik, Phys. Chem. Chem. Phys. **11**, 3861 (2009).
[29] M. Ceotto, S. Atahan, G. F. Tantardini, and A. Aspuru-Guzik, J. Chem. Phys. **130**, 234113 (2009).
[30] N. Makri and W. H. Miller, J. Chem. Phys. **116**, 9207 (2002).
[31] E. Bukhman and N. Makri, J. Phys. Chem. A **111**, 11320 (2007).
[32] B. B. Issack and P.-N. Roy, J. Chem. Phys. **123**, 84103 (2005).
[33] B. B. Issack and P.-N. Roy, J. Chem. Phys. **126**, 24111 (2007).
[34] B. B. Issack and P.-N. Roy, J. Chem. Phys. **127**, 54105 (2007).
[35] B. B. Issack and P.-N. Roy, J. Chem. Phys. **127**, 144306 (2007).
[36] A. L. Kaledin and W. H. Miller, J. Chem. Phys. **119**, 3078 (2003).
[37] Y. Tawada, T. Tsuneda, S. Yanagisawa, Y. Yanai, and K. Hirao, J. Chem. Phys. **120**, 8425 (2004).
[38] J. P. Perdew, K. Burke, and M. Ernzerhof, Phys. Rev. Lett. **77**, 3865 (1996).
[39] K. Hinsen, J. Comput. Chem. **21**, 79 (2000).
[40] K. Yagi, K. Hirao, T. Taketsugu, M. W. Schmidt, and M. S. Gordon, J. Chem. Phys. **121**, 1383 (2004).
[41] J. O. Jung and R. B. Gerber, J. Chem. Phys. **105**, 10332 (1996).
[42] G. M. Chaban, J. O. Jung, and R. B. Gerber, J. Chem. Phys. **111**, 1823 (1999).
[43] L. Pele, B. Brauer, and R. B. Gerber, Theor. Chem. Acc. **117**, 69 (2007).
[44] Y. Scribano and D. M. Benoit, Chem. Phys. Lett. **458**, 384 (2008).

[45]Y. Scribano, D. M. Lauvergnat, and D. M. Benoit, J. Chem. Phys. **133**, 94103 (2010).
[46]K. G. Kay, Chem. Phys. **322**, 3 (2006).
[47]C. Cohen-Tannoudji, B. Diu, and F. Laloë, *Quantum Mechanics* (Wiley and Hermann, Paris, 1977).
[48]R. Gelabert, X. Giménez, M. Thoss, H. Wang, and W. H. Miller, J. Phys. Chem. A **104**, 10321 (2000).
[49]B. R. Johnson, Chem. Phys. **2**, 381 (1973).
[50]C. C. J. Roothaan, Rev. Mod. Phys. **23**, 69 (1951).
[51]J. S. Binkley, J. A. Pople, and W. J. Hehre, J. Am. Chem. Soc. **102**, 939 (1980).
[52]G. H. Peslherbe and W. L. Hase, J. Chem. Phys. **104**, 7882 (1996).
[53]M. W. Schmidt, K. K. Baldridge, J. A. Boatz, S. T. Elbert, M. S. Gordon, J. H. Jensen, S. Koseki, N. Matsunaga, K. A. Nguyen, S. J. Su, T. L. Windus, M. Dupuis, and J. A. Montgomery, J. Comput. Chem. **14**, 1347 (1993).
[54]W. C. Swope, H. C. Andersen, P. H. Berens, and K. R. Wilson, J. Chem. Phys. **76**, 637 (1982).
[55]G. C. Carney, L. L. Sprandel, and C. W. Kern, Adv. Chem. Phys. **37**, 305 (1978).
[56]J. M. Bowman, J. Chem. Phys. **68**, 608 (1978).
[57]J. M. Bowman, K. M. Christoffel, and F. L. Tobin, J. Phys. Chem. **83**, 905 (1979).
[58]K. M. Christoffel and J. M. Bowman, Chem. Phys. Lett. **85**, 220 (1982).
[59]S. Carter, J. M. Bowman, and N. C. Handy, Theor. Chem. Acc. **100**, 191 (1998).
[60]E. R. Davidson, J. Comput. Phys. **17**, 87 (1975).
[61]E. R. Davidson, Comput. Phys. Commun. **53**, 49 (1989).
[62]C. W. Murray, S. C. Racine, and E. R. Davidson, J. Comput. Phys. **103**, 382 (1992)